



UDC 669.2/.8

DOI 10.17073/0368-0797-2024-4-401-408



Original article

Оригинальная статья

## PHASE COMPOSITION AND MICROSTRUCTURE OF INTERMETALLIC ALLOYS OBTAINED USING ELECTRON-BEAM ADDITIVE MANUFACTURING

S. V. Astafurov, E. V. Mel'nikov, E. G. Astafurova , E. A. Kolubaev

Institute of Strength Physics and Materials Science, Siberian Branch of the Russian Academy of Sciences (2/4 Akademicheskii Ave., Tomsk 634055, Russian Federation)

 elena.g.astafurova@ispms.ru

**Abstract.** The paper investigates the microstructure and phase composition of nickel- and aluminum-based intermetallic alloys obtained using two-wire electron-beam additive manufacturing (EBAM). Relevance of the research is related to the widespread use of intermetallic alloys based on nickel and aluminum (mainly  $\text{Ni}_3\text{Al}$ ) in various high-temperature applications and the need to use modern production methods when creating machine parts and mechanisms from these alloys. Using EBAM, the billets from intermetallic alloys with different ratios of the content of main components were obtained. Change in concentrations of the basic elements was carried out varying the ratio of feed rates of nickel and aluminum wires during additive manufacturing in the range from 1:1 to 3:1, respectively. The results of microscopic studies of the obtained alloys showed that, regardless of nickel content, the obtained alloys are characterized by a large-crystalline structure with grain sizes in the range of 100 – 300  $\mu\text{m}$  for alloys with a component ratio of 1:1 and 150 – 400  $\mu\text{m}$  for alloys with a component ratio of 2:1 and 3:1. At the same time, the alloy with an equal content of base components is characterized by more uniform grain and microstructure compared to those with high content of Ni. By changing the concentration ratio of the components, phase composition of the resulting billet can be purposefully controlled. In the case of an “equiatomic” content of the base components in the alloy, a NiAl-based compound with a small phase content based on the intermetallides  $\text{Ni}_3\text{Al}_5$  and  $\text{Ni}_3\text{Al}$  is formed. At high concentrations of nickel, the intermetallic  $\text{Ni}_3\text{Al}$  phase is formed, and at a component ratio of 3:1, structure of the resulting billet consists mainly of  $\text{Ni}_3\text{Al}$  phase and the  $\gamma$  solid substitutional solution based on nickel. The paper demonstrates the possibility of direct production of intermetallic alloys with a given phase composition during electron-beam additive manufacturing.

**Keywords:** intermetallic alloy, additive manufacturing, microstructure, phase composition

**Acknowledgements:** The work was performed in accordance with the state assignment of the Institute of Strength Physics and Materials Science, Siberian Branch of the Russian Academy of Science, subject no. FWRW-2022-0005. The authors express their gratitude to Cand. Sci. (Phys.-Math.) V.E. Rubtsov and Cand. Sci. (Phys.-Math.) S.Y. Nikonov for their assistance in additive manufacturing of the alloys. The research was carried out using the equipment of the Nanotech Research Center (Institute of Strength Physics and Materials Science, Siberian Branch of Russian Academy of Sciences, Tomsk).

**For citation:** Astafurov S.V., Mel'nikov E.V., Astafurova E.G., Kolubaev E.A. Phase composition and microstructure of intermetallic alloys obtained using electron-beam additive manufacturing. *Izvestiya. Ferrous Metallurgy*. 2024;67(4):401–408.

<https://doi.org/10.17073/0368-0797-2024-4-401-408>

## ФАЗОВЫЙ СОСТАВ И МИКРОСТРУКТУРА ИНТЕРМЕТАЛЛИЧЕСКИХ СПЛАВОВ, ПОЛУЧЕННЫХ МЕТОДОМ ПРОВОЛОЧНОГО ЭЛЕКТРОННО-ЛУЧЕВОГО АДДИТИВНОГО ПРОИЗВОДСТВА

С. В. Астафуров, Е. В. Мельников, Е. Г. Астафурова , Е. А. Колубаев

Институт физики прочности и материаловедения Сибирского отделения РАН (Россия, 634055, Томск, пр. Академический, 2/4)

 elena.g.astafurova@ispms.ru

**Аннотация.** В работе проведено исследование микроструктуры и фазового состава интерметаллических сплавов на основе никеля и алюминия, полученных с использованием двухпроволочного электронно-лучевого аддитивного производства (ЭЛАП). Актуальность проведенных исследований связана с широким использованием интерметаллических сплавов на основе никеля и алюминия (преимущественно  $\text{Ni}_3\text{Al}$ ) в различных высокотемпературных приложениях и необходимостью использования современных методов производства

при создании деталей машин и механизмов из этих сплавов. С помощью ЭЛАП были получены заготовки интерметаллических сплавов с разным отношением содержания основных компонентов. Изменение концентрации базовых элементов осуществлялось путем изменения соотношения скоростей подачи никелевой и алюминиевой проволок в процессе аддитивного производства в диапазоне от 1:1 до 3:1 соответственно. Результаты микроскопических исследований полученных сплавов показали, что независимо от содержания никеля полученные сплавы характеризуются крупнокристаллической структурой с размерами зерен в диапазоне 100 – 300 мкм для сплавов с соотношением компонентов 1:1 и 150 – 400 мкм для сплавов с соотношением компонентов 2:1 и 3:1. При этом сплав с равным содержанием базовых компонентов характеризуется более однородной зеренной микроструктурой по сравнению со сплавами с высоким содержанием никеля. При изменении соотношения концентрации компонентов, подаваемых в процессе аддитивного производства, можно целенаправленно управлять фазовым составом получаемой заготовки. В случае «эквивалентного» содержания в сплаве базовых компонентов формируется соединение на основе NiAl с небольшим содержанием фаз на основе интерметаллидов  $Ni_3Al_5$  и  $Ni_3Al$ . При больших концентрациях никеля формируется интерметаллидная фаза  $Ni_3Al$ , а при соотношении компонентов 3:1 структура получаемой заготовки состоит преимущественно из фазы  $Ni_3Al$  и  $\gamma$  твердого раствора замещения на основе никеля. В работе продемонстрирована возможность прямого получения интерметаллических сплавов с заданным фазовым составом в процессе электронно-лучевого аддитивного производства.

**Ключевые слова:** интерметаллический сплав, аддитивное производство, микроструктура, фазовый состав

**Благодарности:** Работа выполнена в рамках госзадания Института физики прочности и материаловедения Сибирского отделения РАН, тема номер FWRW-2022-0005. Авторы выражают благодарность к.ф.-м.н. В.Е. Рубцову и к.ф.-м.н. С.Ю. Никонову за помощь в аддитивном производстве сплавов. Исследования проведены с использованием оборудования ЦКП «Нанотех» (Институт физики прочности и материаловедения Сибирского отделения РАН, Томск).

**Для цитирования:** Астафуров С.В., Мельников Е.В., Астафурова Е.Г., Колубаев Е.А. Фазовый состав и микроструктура интерметаллических сплавов, полученных методом проволочного электронно-лучевого аддитивного производства. *Известия вузов. Черная металлургия*. 2024;67(4):401–408. <https://doi.org/10.17073/0368-0797-2024-4-401-408>

## INTRODUCTION

Intermetallic alloys are solid materials composed of two or more metallic elements [1]. Unlike traditional alloys, intermetallics feature an ordered crystal structure with strong ionic or covalent bonds [1; 2]. These characteristics give intermetallic compounds a range of unique physical and mechanical properties, including high melting points and exceptional strength, even at extremely high temperatures [1; 2].

One of the most intriguing intermetallic compounds for industrial applications is the  $Ni_3Al$  alloy. It boasts high tensile and compressive strength across a broad temperature range, up to 1100 °C [3 – 5], a positive temperature dependence of yield strength between 0 and 800 – 900 °C [3 – 5], and excellent resistance to corrosion, fatigue, creep, and wear, even at elevated temperatures [6 – 8]. These unique properties make nickel and aluminum-based alloys highly valuable in various industries for high-temperature applications, particularly in the production of gas turbine engine blades, turbocharger rotors for diesel power plants, and structural components in the automotive, aerospace, metallurgical, and metalworking sectors [2; 3; 9].

However, these alloys have significant drawbacks, including low plasticity and a tendency toward brittle fracture, which complicates their processing during manufacturing [1; 4; 5]. Traditional powder metallurgy methods – such as casting, sintering, self-propagating high-temperature synthesis, and directional solidification [7; 9; 10] – are not suitable for producing finished products from intermetallic alloys [11 – 13]. As a result, additive manufacturing has emerged as a promising method for producing machine and mechanism parts from nickel aluminide. This process involves creating

a part with a specified shape by sequentially layering and melting powder raw materials or wire using a high-energy beam [10; 11; 14].

In [11], intermetallic alloys with a composite structure were produced using selective laser sintering (SLS) with various mass ratios of aluminum and nichrome alloy powders. The resulting matrix, based on nichrome, was filled with intermetallic particles of  $Ni_3Al$  and NiAl. In [15], layered intermetallic structures based on nickel and aluminum with various stoichiometric compositions were obtained using selective laser melting (SLM) technology. In [16], samples of  $Ni_3Al$  intermetallic alloy were produced using SLM and direct laser metal deposition (DLMD) methods, exhibiting slight microporosity and microcracks that formed during the cooling of the billets. Notably, the samples produced by SLS showed smaller grain sizes compared to those formed during DLMD additive manufacturing, which is attributed to the different heating and cooling regimes in the additive manufacturing process. The cracking of additive intermetallic billets can be avoided by preheating the powder mixture to 1100 °C [13]. In [17], selective electron-beam melting (SEBM) of the IC21 intermetallic alloy powder, based on nickel and aluminum, resulted in a material with a structure free of pores and predominantly consisting of the  $\gamma'$  phase of  $Ni_3Al$ . The alloy demonstrated high strength properties across a wide temperature range (25 – 1000 °C). When forming billets of the IC21 alloy using SLM technology, samples with a dendritic structure were obtained, consisting mainly of the  $\gamma'$  phase of  $Ni_3Al$ , with  $\gamma$ -phase and NiMo-phase grains in the dendrites and interdendritic spaces, respectively [18]. The significant cracking observed in the billets during their crystallization process was also highlighted in.

The primary drawbacks of using additive technologies based on dispersed powders as raw materials include the high cost of powders, their rapid oxidation, and low deposition rates, among other issues [12]. A solution to these problems is to use additive manufacturing methods that employ one or more metallic wires of a specified composition as the raw material. In [12], intermetallic alloys were produced using the wire and arc additive manufacturing (WAAM) method, utilizing nickel and aluminum wires. The refractory nickel wire was melted by an electric arc source, while the low-melting aluminum wire was added directly to the melt bath. It was shown that by adjusting the wire feed rates, the phase composition of the resulting compounds ( $\text{Ni}_3\text{Al}$ ,  $\text{NiAl}$ , etc.) could be altered. In [14; 19], M. Zhang and co-authors demonstrated that when using a two-wire feed in WAAM, a dendritic  $\gamma + \gamma'$  structure with  $\gamma'$ -phase layers in the interdendritic spaces of the  $\text{Ni}_3\text{Al}$  intermetallic alloy forms, and the strength of the resulting billets is comparable to commercial alloys.

Despite its high productivity and the absence of a need for complex and expensive equipment, a drawback of the WAAM method is that the additive manufacturing process occurs in an inert gas environment, which does not fully protect the product from harmful impurities and oxidation. From this perspective, the most effective approach is to use additive technologies where the billets are printed in a vacuum. Such methods include electron-beam additive manufacturing (EBAM) [20].

This study focuses on investigating the structure and phase composition of nickel- and aluminum-based intermetallic alloys produced using EBAM with aluminum and nickel wires.

## EXPERIMENTAL METHODOLOGY

In this study, billets in the form of vertical walls with dimensions of  $120 \times 24 \times 7$  mm and made of nickel and aluminum-based alloys, were produced using a laboratory electron-beam additive manufacturing (EBAM) setup developed in the Institute of Strength Physics and Materials Science SB RAS. To produce the billets, two wires with a diameter of 1.2 mm – nickel (NP-2 alloy, 99.5 wt. % Ni) and aluminum (ESAB OK Autrod 1070 alloy, 99.8 wt. % Al) – were fed into the melt bath. The additive manufacturing process was carried out under the following parameters: beam current ( $I$ ) of  $30 \div 35$  mA, beam scanning speed ( $V_b$ ) of 2.5 mm/s along the deposited layer, accelerating voltage ( $U$ ) of 30 kV, elliptical beam scan from the center, and a scan frequency of 100 Hz. The process was conducted in a vacuum at a pressure of  $10^{-3}$  Pa. The billets were formed by sequential deposition of layers of uniform thickness onto a mild steel substrate. To obtain intermetallic alloys with varying volumetric contents of components, the feed rate ratios

of the nickel and aluminum wires were adjusted, resulting in billets with the following nickel-to-aluminum ratios: 1:1 ( $\text{Ni} + \text{Al}$ ), 2:1 ( $2\text{Ni} + \text{Al}$ ), and 3:1 ( $3\text{Ni} + \text{Al}$ ).

Samples for structural and mechanical studies were cut from the cross-sections of the billets. For microstructural and phase analysis, the samples were mechanically polished, then electrolytically grinded in a solution of 25 g  $\text{CrO}_3$  and 210 ml  $\text{H}_3\text{PO}_4$ , and finally etched in a solution of 90 %  $\text{CH}_3\text{COOH}$  and 10 %  $\text{HClO}_4$ . The microstructure was examined using optical microscopy (OM, Altami MET 1C) and scanning electron microscopy (SEM, Zeiss Leo Evo 50 with an energy-dispersive X-ray spectroscopy (EDS) attachment). X-ray structural and phase analyses were conducted using a Dron-3M diffractometer (Burevestnik) with  $\text{CoK}_\alpha$  radiation. The lattice parameters of the phases were determined by extrapolating the dependence of the ( $ahkl$ ), values, determined for each X-ray line with indices ( $hkl$ ), on the function ( $\cos\theta \cot\theta$ ) [21].

## RESULTS AND DISCUSSION

### Microstructure of alloys produced by EBAM

Fig. 1 presents OM and SEM images of the microstructure of nickel and aluminum-based intermetallic alloys produced using EBAM technology. Metallographic analysis revealed that the billets were free of macro- and microscopic pores or cracks. All three alloys exhibited a coarse-grained layered structure. Within the grains, a dendritic microstructure of different morphology often became visible during electrolytic polishing: depending on the grain orientation relative to the polished surface, either extended, wellformed dendritic branches or broken or partially dissolved dendritic lamellae could be observed. Additionally, homogeneous contrast areas (layers) were noted in the images, where no segregation was detected (Fig. 1).

The  $\text{Ni} + \text{Al}$  alloy demonstrated a fairly homogeneous structure with infrequent interlayers. On a macroscopic level, its structure was more uniform than that of the  $2\text{Ni} + \text{Al}$  and  $3\text{Ni} + \text{Al}$  alloys in terms of forming a layered structure. Meanwhile, the intragranular microstructure of the equiatomic alloy showed little variation along the height of the billet (Fig. 1, *a, b*). Most often, equiaxed grains ranging from 100 to 300  $\mu\text{m}$  in size were observed (Fig. 1, *a, b*). The  $2\text{Ni} + \text{Al}$  and  $3\text{Ni} + \text{Al}$  alloys were characterized by a more heterogeneous structure, with relatively thick interlayers (up to 200  $\mu\text{m}$  thick) and grains elongated in the direction of billet growth (Fig. 1, *c – e*), with grain sizes ranging from 150 to 400  $\mu\text{m}$ . Notably, in alloys with higher nickel content, the dendrites were narrower, and their branches were often intact, indicating a significantly higher density of dendrite/interdendritic boundaries compared to the  $\text{Ni} + \text{Al}$  alloy.

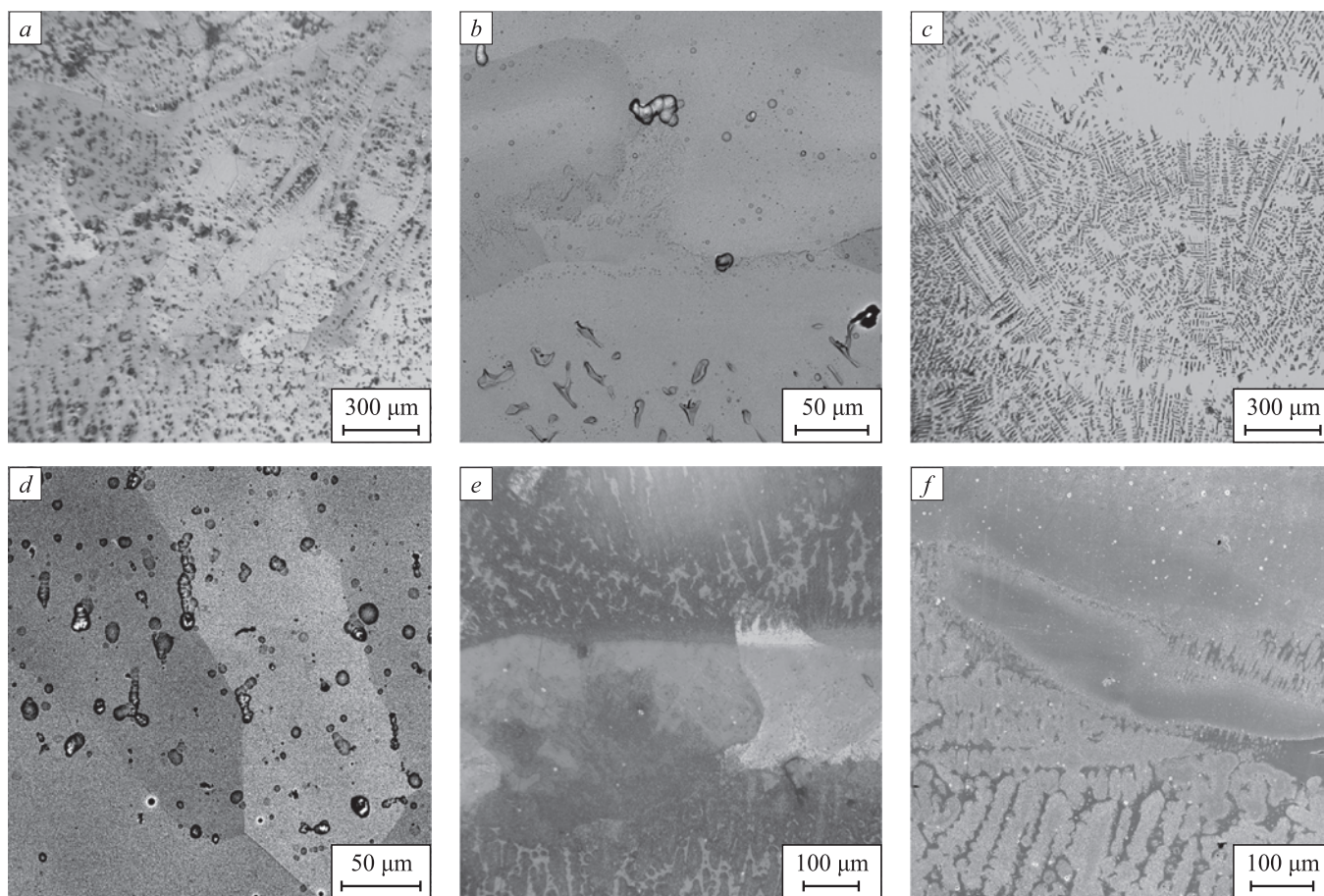


**Fig. 1.** Metallographic (a, c, e) and scanning electron microscopy (b, d, f) images of microstructure of Ni + Al (a, b), 2Ni + Al (c, d) and 3Ni + Al (e, f) intermetallic alloys

**Рис. 1.** ОМ (a, c, e) и СЭМ (b, d, f) изображения микроструктуры интерметаллических сплавов Ni + Al (a, b), 2Ni + Al (c, d) и 3Ni + Al (e, f)

Thus, using two-wire feed EBAM with an equal component ratio results in a homogeneous billet (in terms of microstructure) that is free of macro- and microscopic defects (pores, cracks, etc.) immediately after additive manufacturing.

### Phase composition of alloys obtained by EBAM

According to the phase diagram of the nickel – aluminum system, alloys within this binary system can exist in the following phase states [22 – 24]:

- NiAl<sub>3</sub> (orthorhombic lattice, nickel content: 25 at. %);
- Ni<sub>2</sub>Al<sub>3</sub> (trigonal crystal lattice, homogeneity range for nickel: 37 – 41 at. %);
- NiAl (BCC lattice, homogeneity range for nickel: 42 – 69 at. %);
- Ni<sub>5</sub>Al<sub>3</sub> (orthorhombic crystal lattice, homogeneity range for nickel: 64 – 68 at. %);
- Ni<sub>3</sub>Al (γ'-phase with FCC lattice (L<sub>12</sub> superstructure), homogeneity range for nickel: 73 – 75 at. %);

– Ni<sub>3</sub>Al (γ-phase, disordered solid solution with FCC lattice with homogeneity region for nickel: 73 – 75 at. %).

In this study of additive manufacturing of intermetallic alloys, the nickel content fed into the billet during EBAM is relatively high (according to the chemical composition of the NP-2 alloy, not less than 49.5 wt. % for the Ni + Al billet). Therefore, the expected phases in the resulting billets, based on the phase diagram, include NiAl, Ni<sub>5</sub>Al<sub>3</sub>, Ni<sub>3</sub>Al, and a nickel-based alloy enriched with aluminum through a substitution mechanism (when the nickel content in the system exceeds 75 at. %).

X-ray phase and X-ray microanalyses revealed that the phase composition of the billets produced by EBAM is determined by the feed rate ratio of nickel and aluminum wires into the melt bath, or, in other words, by the mass ratio of the components of forming the intermetallic alloy. Figs. 2 and 3 show X-ray patterns and SEM images with marked EDS spectrum areas for the obtained billets. The table provides data on the chemical composition and corresponding phases in different areas of the examined samples (as per Fig. 3), obtained from EDS analysis for the three billets with different compo-

nent ratios of nickel and aluminum (phases were identified based on a comparison of the chemical composition in the EDS spectrum area with the “nickel – aluminum” phase diagram [22 – 24]).

Fig. 2, *a* shows that when the feed rate ratio of the two wires is Ni = 1:1, the resulting billet has a heterophase structure composed of NiAl, Ni<sub>5</sub>Al<sub>3</sub>, and Ni<sub>3</sub>Al phases. However, according to X-ray phase analysis, the Ni<sub>3</sub>Al intermetallic phase is not the predominant phase, and EDS analysis does not detect this phase at all (Fig. 3, *a*, see the Table). Consequently, in the EBAM process, when nickel and aluminum wires are fed into the melt bath at equal speeds, i.e., with a near-equal mass ratio of nickel and aluminum, the formed intermetallic alloy predominantly consists of NiAl and Ni<sub>5</sub>Al<sub>3</sub> phases.

Increasing the wire feed rate ratio to Ni:Al = 2:1 in the EBAM process results in an intermetallic alloy with a more complex phase composition. According to the X-ray phase study (Fig. 2, *b*), the formed billet has a heterophase structure consisting of NiAl, Ni<sub>5</sub>Al<sub>3</sub>, Ni<sub>3</sub>Al, and Ni phases. At the same time, EDS analysis indicates that the main phase in this case is Ni<sub>3</sub>Al, with the content of the other three phases being relatively small (Fig. 2, *b*, see the Table).

Further increasing the wire feed rate ratio to Ni:Al = 3:1 leads to the formation of a two-phase alloy based on Ni and Ni<sub>3</sub>Al (Fig. 2, *c*, Fig. 3, *c*, Table). In this case, the formed Ni<sub>3</sub>Al intermetallic phase has a lattice parameter of  $a = 0.3572$  nm. This value is lower than the typical value for the  $\gamma'$ -phase of  $a = 0.3589$  nm (for the L1<sub>2</sub> superstructure [23]). Such differences may be due to the formation of a two-phase composition ( $\gamma + \gamma'$ ) in the Ni<sub>3</sub>Al grains during EBAM, i.e., the formation of regions of disordered  $\gamma'$ -solid solution based on Ni<sub>3</sub>Al together with the ordered  $\gamma$ -phase. On the other hand, the lattice parameter of Ni in the formed alloy is higher than that of pure FCC nickel ( $a = 0.3568$  nm vs.  $a = 0.3526$  nm [25]). This may be due to the formation of a solid solution of aluminum in nickel via the substitution mechanism.

The results of X-ray phase analysis and energy-dispersive spectroscopy (EDS) of the intermetallic alloys produced by EBAM showed that their phase composition generally corresponds to the mass ratio of the initial materials (nickel and aluminum wires) fed into the melt bath during additive manufacturing. For instance, with a Ni ratio of 1:1, the primary phase is NiAl; at a ratio of 2:1, a significant portion of the Ni<sub>3</sub>Al phase is formed, with the excess aluminum being redistributed to form Ni<sub>5</sub>Al<sub>3</sub> grains. When the nickel content is three times that of aluminum, the primary phase is Ni<sub>3</sub>Al. Moreover, X-ray phase and EDS analyses did not detect any unreacted aluminum in the resulting alloys, indicating that all the alu-

minum was fully incorporated into the formation of intermetallic compounds during the EBAM process.

Thus, the study results demonstrate that the EBAM process allows for the formation of nickel- and alumi-

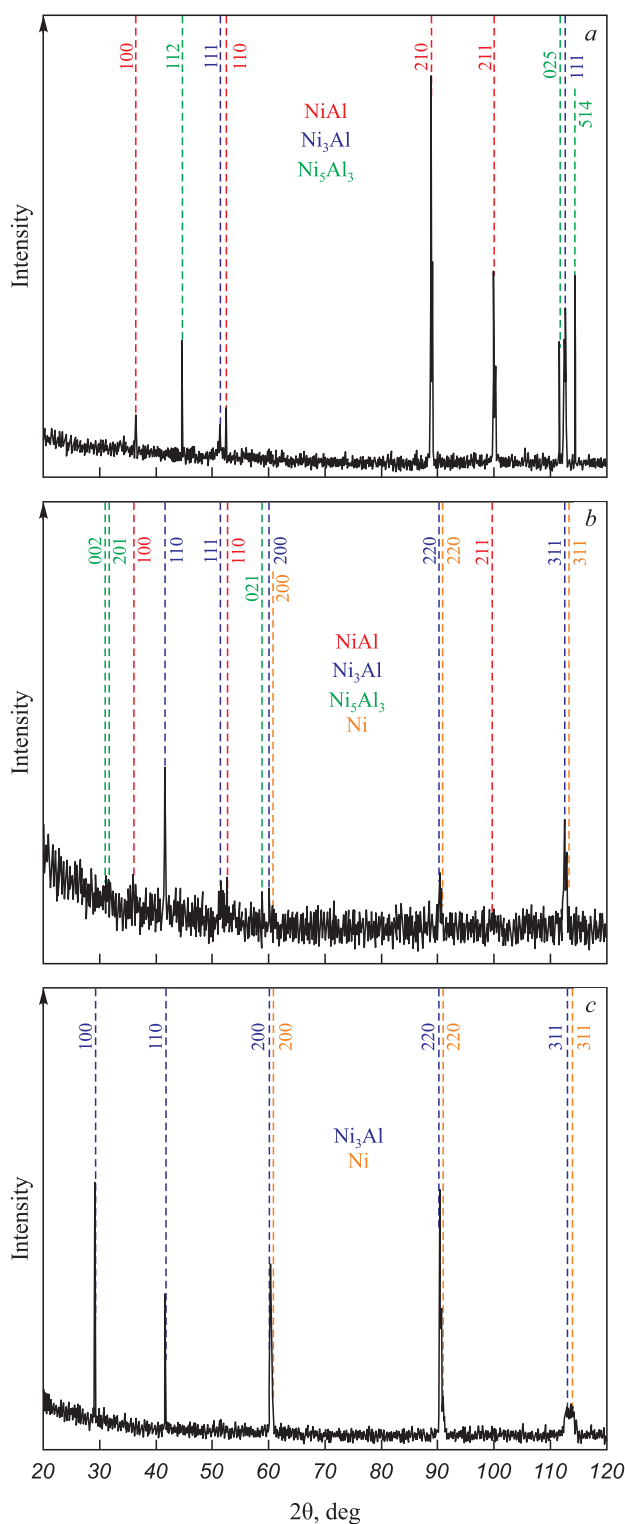


**Fig. 2.** XRD-patterns of intermetallic alloys Ni + Al, 2Ni + Al and 3Ni + Al ( $a - c$ )

**Рис. 2.** Рентгенограммы интерметаллических сплавов Ni + Al, 2Ni + Al и 3Ni + Al ( $a - c$ )

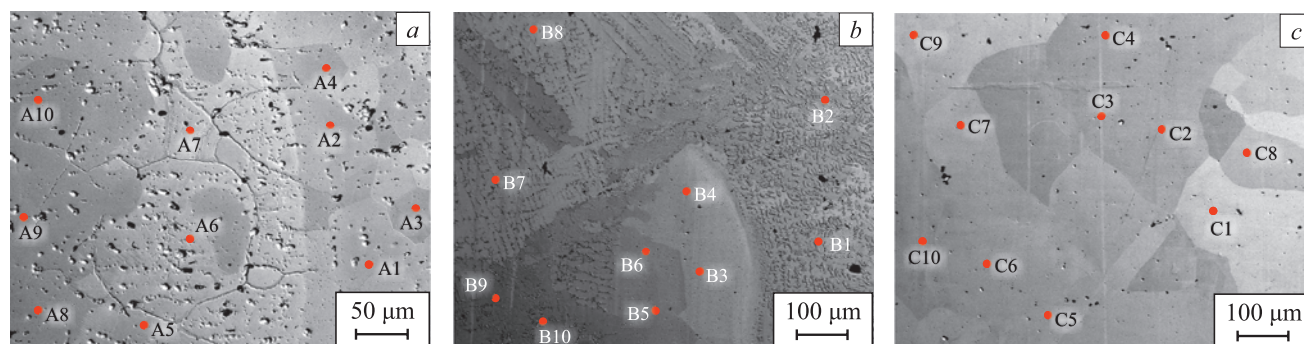


Fig. 3. SEM-images of microstructure of intermetallic alloys Ni + Al, 2Ni + Al and 3Ni + Al (a – c) with EDS spectra positions (Table)

Рис. 3. СЭМ изображения микроструктуры интерметаллических сплавов Ni + Al, 2Ni + Al и 3Ni + Al (a – c) с нанесенными областями определения ЭДС спектров (см. таблицу)

### Chemical and phase composition of intermetallic alloys in the zones of EDS analysis shown in Fig. 3

#### Химический и фазовый составы интерметаллических сплавов в областях проведения ЭДС анализа, обозначенных на рис. 3

Ni:Al = 1:1			Ni:Al = 2:1			Ni:Al = 3:1		
Spectrum	Al/Ni, at. %	Phase	Spectrum	Al/Ni, at. %	Phase	Spectrum	Al/Ni, at. %	Phase
A1	42.5/57.5	NiAl	B1	40.6/59.4	NiAl	C1	18.2/81.8	Ni <sub>3</sub> Al + Ni
A2	41.8/58.2	NiAl	B2	30.6/69.4	Ni <sub>5</sub> Al + Ni <sub>3</sub> Al	C2	16.1/83.9	Ni <sub>3</sub> Al + Ni
A3	42.8/57.2	NiAl	B3	25.9/74.1	Ni <sub>3</sub> Al	C3	15.4/84.6	Ni <sub>3</sub> Al + Ni
A4	40.7/59.3	NiAl	B4	26.3/73.7	Ni <sub>3</sub> Al	C4	15.1/84.9	Ni <sub>3</sub> Al + Ni
A5	35.0/65.0	Ni <sub>5</sub> Al <sub>3</sub>	B5	35.2/64.8	Ni <sub>5</sub> Al <sub>3</sub>	C5	14.9/85.1	Ni <sub>3</sub> Al + Ni
A6	36.1/63.9	Ni <sub>5</sub> Al <sub>3</sub>	B6	22.7/77.3	Ni <sub>3</sub> Al + Ni	C6	14.5/85.5	Ni <sub>3</sub> Al + Ni
A7	36.2/63.8	Ni <sub>5</sub> Al <sub>3</sub>	B7	27.4/72.6	Ni <sub>3</sub> Al	C7	15.1/84.9	Ni <sub>3</sub> Al + Ni
A8	36.3/63.7	Ni <sub>5</sub> Al <sub>3</sub>	B8	26.9/73.1	Ni <sub>3</sub> Al	C8	18.8/81.2	Ni <sub>3</sub> Al + Ni
A9	37.6/62.4	NiAl	B9	26.6/73.4	Ni <sub>3</sub> Al	C9	13.5/86.5	Ni <sub>3</sub> Al + Ni
A10	37.1/62.9	NiAl	B10	46.0/54.0	NiAl	C10	15.3/84.7	Ni <sub>3</sub> Al + Ni

num-based intermetallic alloys with a predetermined phase composition by varying the mass ratio of the components fed into the melt bath.

### CONCLUSIONS

Using EBAM technology with a two-wire feed, billets of nickel- and aluminum-based intermetallic alloys with varying component contents were produced. The mass ratio of nickel to aluminum was adjusted by varying the feed rates of the two wires into the melt bath during the additive manufacturing process. The resulting billets were characterized by a coarse-grained, layered structure. The alloy with an equal content of nickel and aluminum exhibited a more homogeneous internal structure compared to the alloys with ratios of 2:1 and 3:1.

The phase composition of the resulting alloys was also determined by the mass ratio of the components used in the additive manufacturing process. When the wire

feed rate ratio was 1:1, a NiAl-based alloy was formed with a small content of Ni<sub>3</sub>Al<sub>5</sub> and Ni<sub>3</sub>Al phases. Increasing the nickel content alters the phase composition of the intermetallic alloy, and at a nickel-to-aluminum ratio of 3:1, the structure of the resulting billet predominantly consists of (γ + γ') Ni<sub>3</sub>Al and a γ-substitutional solid solution based on nickel with a small amount of aluminum.

The results of this study demonstrated the fundamental possibility of producing nickel- and aluminum-based intermetallic alloys with a specified chemical composition using EBAM technology.

### REFERENCES / СПИСОК ЛИТЕРАТУРЫ

- Jozwik P., Polkowski W., Bojar Z. Applications of Ni<sub>3</sub>Al based intermetallic alloys – current stage and potential perspectives. *Materials*. 2015;8(5):2537–2568. <https://doi.org/10.3390/ma8052537>

2. Westbrook J.H., Fleischer R.L. Structural Applications of Intermetallic Compounds. Vol. 3. New York: John Wiley and Son Ltd.; 2000:292.
3. Bochenek K., Basista M. Advances in processing of NiAl intermetallic alloys and composites for high temperature aerospace applications. *Progress in Aerospace Sciences*. 2015;79: 136–146. <https://doi.org/10.1016/j.paerosci.2015.09.003>
4. Iwabuchi Y., Kobayashi I. Various properties of dual-phase intermetallic compound in Ni–Al system. *Materials Science*. 2010;638–642:1348–1352. <https://doi.org/10.4028/www.scientific.net/MSF.638-642.1348>
5. Lu Y., Gu J., Kim S., Hong H., Choi H., Lee J. Tensile behavior of directionally solidified Ni<sub>3</sub>Al intermetallics with different Al contents and solidification rates. *Metals and Materials International*. 2014;20:221–2277. <https://doi.org/10.1007/s12540-014-1021-1>
6. Sheng L.Y., Zhang W., Guo J.T., Wang Z.S., Ovcharenko V.E., Zhou L.Z., Ye H.Q. Microstructure and mechanical properties of Ni<sub>3</sub>Al fabricated by thermal explosion and hot extrusion. *Intermetallics*. 2009;17(7):572–577. <https://doi.org/10.1016/j.intermet.2009.01.004>
7. Ovcharenko V.E., Boyangin E.N., Myshlyaev M.M., Ivanov Yu.F., Ivanov K.V. Formation of a multi-grain structure and its influence on strength and plasticity of the Ni<sub>3</sub>Al intermetallic compound. *Fizika tverdogo tela*. 2015;57(7): 1270–1276. (In Russ.)  
Овчаренко В.Е., Боянгин Е.Н., Мышляев М.М., Иванов Ю.Ф., Иванов К.В. Формирование мультigrанной структуры и ее влияние на прочность и пластичность интерметаллического соединения Ni<sub>3</sub>Al. *Физика тverdogo tela*. 2015;57(7):1270–1276.
8. Guo J., Sheng L., Xie Y., Zhang Z., Ovcharenko V., Ye H. Microstructure and mechanical properties of Ni<sub>3</sub>Al and Ni<sub>3</sub>Al-B alloys fabricated by SHS/HE. *Intermetallics*. 2011;19(2):137–142. <https://doi.org/10.1016/j.intermet.2010.08.027>
9. Liu C.T., Sikka V.K. Nickel aluminides for structural use. *JOM*. 1986;38:19–21. <https://doi.org/10.1007/BF03257837>
10. Awotunde M.A., Ayodele O.O., Adegbenjo A.O., Okoro A.M., Shongwe M.B., Olubambi P.A. NiAl intermetallic composites – a review of processing methods, reinforcements and mechanical properties. *The International Journal of Advanced Manufacturing Technology*. 2019;104:1733–1747. <https://doi.org/10.1007/s00170-019-03984-9>
11. Shishkovsky I.V. Laser-controlled intermetallics synthesis during surface cladding. *Laser Surface Engineering*. 2015:237–286. <https://doi.org/10.1016/B978-1-78242-074-3.00011-8>
12. Meng Y., Li J., Gao M., Zeng X. Microstructure characteristics of wire arc additive manufactured Ni – Al intermetallic compounds. *Journal of Manufacturing Processes*. 2021;68(A):932–939. <https://doi.org/10.1016/j.jmapro.2021.06.022>
13. Müller M., Heinen B., Riede M., López E., Brückner F., Leyens C. Additive manufacturing of β-NiAl by means of laser metal deposition of pre-alloyed and elemental powders. *Materials*. 2021;14(9):2246. <https://doi.org/10.3390/ma14092246>
14. Zhang M., Wang Y., Yang Z., Ma Z., Wang Z., Wang D. Microstructure and mechanical properties of twin wire and arc additive manufactured Ni<sub>3</sub>Al-based alloy. *Journal of Materials Processing Technology*. 2022;303:117529. <https://doi.org/10.1016/j.jmatprotec.2022.117529>
15. Nazarov A., Safronov V.A., Khmyrov R.S., Shishkovsky I. Fabrication of gradient structures in the Ni – Al system via SLM process. *Procedia IUTAM*. 2017;23:161–166. <https://doi.org/10.1016/j.piutam.2017.06.017>
16. Kotoban D., Nazarov A., Shishkovsky I. Comparative study of selective laser melting and direct laser metal deposition of Ni<sub>3</sub>Al intermetallic alloy. *Procedia IUTAM*. 2017;23: 138–146. <https://doi.org/10.1016/j.piutam.2017.06.014>
17. Yao Y., Xing C., Peng H., Guo H., Chen B. Solidification microstructure and tensile deformation mechanisms of selective electron beam melted Ni<sub>3</sub>Al-based alloy at room and elevated temperatures. *Materials Science and Engineering: A*. 2021;802:140629. <https://doi.org/10.1016/j.msea.2020.140629>
18. Chai H., Wang L., Lin X., Zhang S., Yang H., Huang W. Microstructure and cracking behavior of Ni<sub>3</sub>Al-based IC21 alloy fabricated by selective laser melting. *Materials Characterization*. 2023;196:112592. <https://doi.org/10.1016/j.matchar.2022.112592>
19. Zhang M., Wang Y., Ma Z., Wang Z., Yang Z. Non-uniform high-temperature oxidation behavior of twin wire and arc additive manufactured Ni<sub>3</sub>Al-based alloy. *Journal of Manufacturing Processes*. 2022;84:522–530. <https://doi.org/10.1016/j.jmapro.2022.10.035>
20. Kolubaev E.A., Rubtsov V.E., Chumaevsky A.V., Astafurova E.G. Micro-, meso- and macrostructural design of bulk metallic and polymetallic materials by wire-feed electron-beam additive manufacturing. *Physical Mesomechanics*. 2022;25:479–491. <https://doi.org/10.1134/S1029959922060017>
21. Naidu S.V.N., Singh T. X-ray characterization of eroded 316 stainless steel. *Wear*. 1993;166(2):141–145. [https://doi.org/10.1016/0043-1648\(93\)90255-K](https://doi.org/10.1016/0043-1648(93)90255-K)
22. Lyakishev N.P. State Diagrams of Double Metal Systems; Handbook. Vol. 1. Moscow: Mashinostroenie; 1997:1024. (In Russ.)  
Лякишев Н.П. Диаграммы состояния двойных металлических систем. Т. 1. Москва: Машиностроение; 1997:1024.
23. Kovtunov A.I., Myamin S.V. Intermetallic Alloys: An electronic textbook. Tolyatti: Izd-vo TSU; 2018:77. (In Russ.)  
Ковтунов А.И., Мямин С.В. Интерметаллидные сплавы. Тольятти: Изд-во ТГУ; 2018:77.
24. Nash P., Singleton M.F., Murray J.L. Phase Diagrams of Binary Nickel Alloys. ASM International, Materials Park, OH; 1991:3–11.
25. Hermann K. Crystallography and Surface Structure: An Introduction for Surface Scientists and Nanoscientists. Weinheim: Wiley; 2011:298. <http://dx.doi.org/10.1002/9783527633296>

## Information about the Authors

## Сведения об авторах

**Sergei V. Astafurov**, *Cand. Sci. (Phys.-Math.), Senior Researcher of the Laboratory of Physics of Hierarchical Structures in Metals and Alloys, Institute of Strength Physics and Materials Science, Siberian Branch of Russian Academy of Sciences*

**ORCID:** 0000-0003-3532-3777

**E-mail:** svastafurov@gmail.com

**Evgenii V. Mel'nikov**, *Junior Researcher of the Laboratory of Physics of Hierarchical Structures in Metals and Alloys, Institute of Strength Physics and Materials Science, Siberian Branch of Russian Academy of Sciences*

**ORCID:** 0000-0001-8238-6055

**E-mail:** melnickow-jenya@yandex.ru

**Elena G. Astafurova**, *Dr. Sci. (Phys.-Math.), Assist. Prof., Head of the Laboratory of Physics of Hierarchical Structures in Metals and Alloys, Institute of Strength Physics and Materials Science, Siberian Branch of Russian Academy of Sciences*

**ORCID:** 0000-0002-1995-4205

**E-mail:** elena.g.astafurova@ispms.ru

**Evgenii A. Kolubaev**, *Dr. Sci. (Eng.), Director, Institute of Strength Physics and Materials Science, Siberian Branch of the Russian Academy of Sciences*

**ORCID:** 0000-0001-7288-3656

**E-mail:** eak@ispms.ru

**Сергей Владимирович Астафуров**, *к.ф.-м.н., старший научный сотрудник лаборатории физики иерархических структур в металлах и сплавах, Институт физики прочности и материаловедения Сибирского отделения РАН*

**ORCID:** 0000-0003-3532-3777

**E-mail:** svastafurov@gmail.com

**Евгений Васильевич Мельников**, *младший научный сотрудник лаборатории физики иерархических структур в металлах и сплавах, Институт физики прочности и материаловедения Сибирского отделения РАН*

**ORCID:** 0000-0001-8238-6055

**E-mail:** melnickow-jenya@yandex.ru

**Елена Геннадьевна Астафурова**, *д.ф.-м.н., доцент, заведующий лабораторией физики иерархических структур в металлах и сплавах, Институт физики прочности и материаловедения Сибирского отделения РАН*

**ORCID:** 0000-0002-1995-4205

**E-mail:** elena.g.astafurova@ispms.ru

**Евгений Александрович Колубаев**, *д.т.н., директор, Институт физики прочности и материаловедения Сибирского отделения РАН*

**ORCID:** 0000-0001-7288-3656

**E-mail:** eak@ispms.ru

## Contribution of the Authors

## Вклад авторов

**S. V. Astafurov** – literary review, microstructural studies, analysis of results, X-ray studies, writing the text, design of the article.

**E. V. Mel'nikov** – literary review, sample preparation, analysis and graphical representation of results.

**E. G. Astafurova** – scientific guidance, reviewing and editing of the final version of the article.

**E. A. Kolubaev** – scientific guidance, reviewing and editing of the final version of the article.

**С. В. Астафуров** – обзор литературы, проведение микроструктурных исследований, проведение рентгеновских исследований, анализ результатов, написание текста рукописи, оформление статьи.

**Е. В. Мельников** – обзор литературы, подготовка образцов, анализ и графическое представление полученных результатов.

**Е. Г. Астафурова** – научное руководство исследованиями, редактирование финальной версии статьи.

**Е. А. Колубаев** – научное руководство, редактирование финальной версии статьи.

Received 21.06.2023

Revised 10.01.2024

Accepted 20.05.2024

Поступила в редакцию 21.06.2023

После доработки 10.01.2024

Принята к публикации 20.05.2024